1521-0103/346/1/31–37$25.00
THE JOURNAL OF PHARMACOLOGY AND EXPERIMENTAL THERAPEUTICS

http://dx.doi.org/10.1124/jpet.112.202275
J Pharmacol Exp Ther 346:31–37, July 2013

Pivotal Role of Mouse Mast Cell Protease 4 in the Conversion and Pressor Properties of Big-Endothelin-1[S]

Martin Houde, Marc-David Jamain, Julie Labonté, Louisane Desbiens, Gunnar Pejler, Michael Gurish, Shinji Takai, and Pedro D'Orléans-Juste

Department of Pharmacology, Université de Sherbrooke, Sherbrooke, Quebec, Canada (M.H., M.-D.J., J.L., L.D., P.D.-J.); Department of Anatomy, Physiology and Biochemistry, Swedish University of Agricultural Sciences, Uppsala, Sweden (G.P.); Department of Medicine, Brigham and Women's Hospital, Harvard University, Boston, Massachusetts (M.G.); and Department of Pharmacology, Osaka Medical College, Osaka, Japan (S.T.)

Received December 3, 2012; accepted April 15, 2013

ABSTRACT

The serine protease chymase has been reported to generate intracardiac angiotensin-II (Ang-II) from Ang-I as well as an intermediate precursor of endothelin-1 (ET-1), ET-1 (1–31) from Big-ET-1. Although humans possess only one chymase, several murine isoforms are documented, each with its own specific catalytic activity. Among these, mouse mast cell protease 4 (mMCP-4) is the isoform most similar to the human chymase for its activity. The aim of this study was to characterize the capacity of mMCP-4 to convert Big-ET-1 into its bioactive metabolite, ET-1, in vitro and in vivo in the mouse model. Basal mean arterial pressure did not differ between wild-type (WT) and mMCP-4(−/−) mice. Systemic administration of Big-ET-1 triggered pressor responses and increased blood levels of immunoreactive (IR) ET-1 (1–31) and ET-1 that were reduced by more than 50% in mMCP-4 knockout (−/−) mice compared with WT controls. Residual responses to Big-ET-1 in mMCP-4(−/−) mice were insensitive to the enkephalinase/neutral endopeptidase inhibitor thiorphan and the specific chymase inhibitor TY-51469 {2-[4-(5-fluoro-3-methylbenzo[b]thiophen-2-yl)sulfonamido-3-methanesulfonylphenyl]thiazole-4-carboxylic acid}. Soluble fractions from the lungs, left cardiac ventricle, aorta, and kidneys of WT but not mMCP-4(−/−) mice generated ET-1 (1–31) from exogenous Big-ET-1 in a TY-51469-sensitive fashion as detected by high-performance liquid chromatography/ matrix-assisted laser desorption/ionization-mass spectrometry. Finally, pulmonary endogenous levels of IR-ET-1 were reduced by more than 40% in tissues derived from mMCP-4(−/−) mice compared with WT mice. Our results show that mMCP-4 plays a pivotal role in the dynamic conversion of systemic Big-ET-1 to ET-1 in the mouse model.

Introduction

In the human cardiovascular system, mast cell-derived serine protease chymase generates the vasoconstrictor peptide angiotensin II (Ang-II), especially in the heart and the vascular wall (Urata et al., 1993; Mangiapane et al., 1994). Chymase, similarly to the angiotensin converting enzyme, cleaves the precursor angiotensin-I to yield the biologically active Ang-II (Urata et al., 1990). Pivotal roles of chymase have also been demonstrated in several animal models of cardiovascular diseases, such as atherosclerosis, many of them in relation to its Ang-II producing activity (Fleming, 2006). For instance, chymase presence is increased in the atherosclerotic plaque (Kaartinen et al., 1994), and the inhibition of chymase reduces the size of Ang-II-induced abdominal aneurysms in the mouse (Inoue et al., 2009).

Endothelin-1 (ET-1), on the other hand, is a 21 amino acid peptide (Yanagisawa et al., 1988) that exerts its actions via two receptors, ET_A and ET_B (Arai et al., 1990; Sakurai et al., 1990). ET-1 is derived from proendothelin-1, which is cleaved by furin to yield a 38 amino acid intermediate, Big-ET-1 (Denault et al., 1995). Big-ET-1 is then hydrolyzed at the Trp^{21}–Val^{22} bond to yield the bioactive ET-1 by an endothelin-converting enzyme (ECE) (McMahon et al., 1991; D'Orleans-Juste et al., 2003).

Mice knocked out for both ECE genes do not survive the late gestational stage, yet embryonic tissues of these mice still retain two-thirds of total endothelin peptides measured in wild-type (WT) congeners (Yanagisawa et al., 2000). Thus, other proteases are involved in the overall production of mature ET-1 in the mouse.

This work was supported by the Canadian Institutes for Health Research [Grant MOP-57883 (to P.D.-J.)]; the National Institutes of Health [Grants R01-AI083516 (to M.G.) and GM 052585-15 (to M.G.)]; as well as by the Etienne Lebel Clinical Research Center of the Centre Hospitalier Universitaire de Sherbrooke. M.H. is in receipt of a Ph.D. scholarship from the Canadian Institutes for Health Research.
dx.doi.org/10.1124/jpet.112.202275.
[S] This article has supplemental material available at jpet.aspetjournals.org.

ABBREVIATIONS: AMC, Suc-Leu-Leu-Val-Tyr-7-amino-4-methylcoumarin; Ang, angiotensin; CGS 35066, (α-[(*S*)-(Phosphonomethyl)amino]-3-dibenzofuranpropanoic acid); CPA, carboxypeptidase A; ECE, endothelin-converting enzyme; ET-1, endothelin-1; EIA, enzyme immunoassay; HPLC, high-performance liquid chromatography; IR, immunoreactive; MALDI, matrix-assisted laser desorption/ionization; mMCP, mouse mast cell protease; MMP, matrix metalloproteinase; MS, mass spectrometry; NEP, neutral endopeptidase 24.11; PCR, polymerase chain reaction; TY-51469, 2-[4-(5-fluoro-3-methylbenzo[b]thiophen-2-yl)sulfonamido-3-methanesulfonylphenyl]thiazole-4-carboxylic acid; WT, wild-type.

The first report of non-ECE-dependent synthesis of ET-1 from Big-ET-1 showed that chymostatin, a nonspecific inhibitor of chymotrypsin-like proteases, efficiently blocked the processing of Big-ET-1 into its active metabolite in perfused rat lungs (Wypij et al., 1992). Chymase has subsequently been reported to hydrolyze Big-ET-1 to a 31 amino acid peptide, ET-1 (1–31) (Hanson et al., 1997; Nakano et al., 1997). Initially reported as a direct ET_A receptor agonist (Yoshizumi et al., 1998), additional in vitro (Hayasaki-Kajiwara et al., 1999) and in vivo studies (Fecteau et al., 2005) showed that ET-1 (1–31) must first be converted by the neutral endopeptidase 24.11 (NEP) to normal-length ET-1 to exert biologic activities. Interestingly, Mawatari et al. (2004) reported high concentrations of ET-1 (1–31) in the atheromas of atherosclerotic patients. More recently, our laboratory demonstrated that specific chymase inhibition markedly reduces the synthesis of ET-1 from exogenous Big-ET-1 in the mouse model in vivo (Simard et al., 2009).

Whereas a single human chymase isoform has been reported, several have been identified in the mouse, each with a distinct activity (Pejler et al., 2010). Among those isoforms, studies on the role of chymase in the synthesis of Ang-II suggest that mouse mast cell protease 4 (mMCP-4) is the murine isoform having the most similar proteolytic activity to that of human chymase (Caughey, 2007; Andersson et al., 2008; D'Orléans-Juste et al., 2008). Whether mMCP-4 is also involved in the generation of ET-1 from its precursor Big-ET-1 has yet to be determined.

Therefore, using mice genetically deficient for mMCP-4 [mMCP-4(−/−)] (Tchougounova et al., 2003) as well as the specific chymase inhibitor TY-51469 (Koide et al., 2003; Palaniyandi et al., 2007), we studied the role of this chymase isoform in the biologic activity of Big-ET-1 in vitro and in vivo. Our results suggest a pivotal role for mMCP-4 in the cardiovascular properties of Big-ET-1.

Materials and Methods

See Supplemental Methods online for additional information.

Animals. C57BL/6J mice were purchased from Charles River (Montréal, QC, Canada) and housed in our facilities. Genitor mMCP-4(−/−) mice (Tchougounova et al., 2003) were bred in our facilities, and their genotype was confirmed by polymerase chain reaction (PCR) (see Supplemental Fig. 1; Supplemental Tables 1 and 2). All animals were kept at constant room temperature (23°C) and humidity (78%) under a controlled light/dark cycle (6:00 AM–6:00 PM), with standard chow and tap water available ad libitum. Animal care and experiments were approved by the Ethics Committee on Animal Research of the Université de Sherbrooke following the Canadian Council on Animal Care guidelines and the Guide for the Care and Use of Laboratory Animals of the United States National Institutes of Health.

All experiments on mice were performed on male mice under general anesthesia, with a mixture of ketamine/xylazine (87/13 mg/kg i.m.) (Bioniche, Belleville, ON, Canada; and Bimeda, Cambridge, ON, Canada). Maintenance anesthesia was performed with one-third of the initial dose every 30 minutes. Complete anesthesia was assumed when no withdrawing reflex was found during pressure on any paw of the mouse. After procedure completion and prior to tissue sampling, anesthetized mice were killed by cervical dislocation.

RNA Extraction and Reverse-Transcription Quantitative PCR. Pulmonary, cardiac, aortic, and renal tissues from C57BL/6J and mMCP-4(−/−) mice were homogenized using a tissue dispersing apparatus ULTRA-TURRAX T8 (IKA Works, Wilmington, NC). The purification of total RNA was carried out on RNeasy columns for fibrous tissues (Qiagen, Toronto, ON, Canada). The protocol was performed as recommended by the manufacturer except for DNAse treatment. Quantitative PCR for actin, ECE-1a, NEP, mMCP-1, carboxypeptidase-A1 (CPA1) was performed by monitoring in real time increase in fluorescence of SYBR Green incorporation (Perfecta SYBR Green SuperMix, low ROX; Quanta Biosciences, Gaithersburg, MD) using the MX3000P Multiplex Quantitative PCR System (Agilent Technologies, Santa Clara, CA). Levels of actin were constant between organs of WT and mMCP4(−/−) mice and used as internal controls for normalization. Fold changes from the WT to mMCP-4(−/−) is determined using the ($2^{-\Delta\Delta CT}$) method (Pfaffl, 2001).

Specific Chymotrypsin-Like Activity In Vitro. WT and mMCP-4(−/−) mice were killed and the lungs, left cardiac ventricle, aorta, and kidneys were homogenized and centrifuged, and the supernatants were collected for the assay. By use of the nonfluorescent substrate Suc-Leu-Leu-Val-Tyr-7-amino-4-methylcoumarin (AMC) (Peptide Institute, Osaka, Japan), fluorescence AMC-forming activity, as chymotrypsin-like activity, was then measured with a fluorescence spectrophotometer (λ_{ex}: 370 nm; λ_{em}: 460 nm) (Molecular Devices, Sunnyvale, CA). Some experiments were performed with pretreatment of the soluble extracts with the specific chymase inhibitor TY-51469 (10 μM) (graciously provided by Toa Eiyo Ltd., Osaka, Japan).

In Vitro Conversion of Big-ET-1 to ET-1 (1–31). Soluble fractions from the lungs, left cardiac ventricle, aorta, and kidneys were collected from WT and mMCP-4(−/−) mice as described above.

The soluble fractions were incubated with Big-ET-1 (7.5 μM), either with vehicle or TY-51469 {2-[4-(5-fluoro-3-methylbenzo[b]thiophen-2-yl)sulfonamido-3-methanesulfonylphenyl]thiazole-4-carboxylic acid} (10 μM), after which samples were filtered through a 30K Amicon centrifugal filter unit (Millipore Corporation, Billireca, MA) for high-performance liquid chromatography (HPLC)- mass spectrometry (MS) analysis. Filtrates were collected and purified by reversed phase HPLC (1100 series) with a Zorbax C-18 analytical column (Agilent Technologies). Quantification was assessed with absorbance at a wavelength of 214 nm and 30-second fractions at the Big-ET-1 and ET-1 (1–31) elution peaks were collected for matrix-assisted laser desorption/ionization (MALDI) mass spectrometry analysis. The MALDI-Time of Flight was performed on a ProteinChip system (Bio-Rad Laboratories Inc., Mississauga, ON, Canada) using a gold plate as support and α-cyano-4-hydroxycinnamic acid (Sigma-Aldrich, St-Louis, MO) as the matrix.

Telemetric Hemodynamic Recording in Conscious Mice. Telemetry probe implantation was achieved in accordance to Carlson and Wyss (2000) and Butz and Davisson (2001). Briefly, anesthetized WT and mMCP-4(−/−) mice were implanted with a catheter-tipped transmitter (TA11PA-C20; Data Sciences International, St. Paul, MN) into the aortic arch. The transmitter was placed subcutaneously along the right flank of the animal. A buprenorphine protocol of 0.1 mg/kg every 9 hours for 24 hour postoperation was conducted to control surgical pain. The mice had a 14-day recovery period before recording of hemodynamic data. The mice were then monitored at 15-minute intervals for 24 hours via Acquisition Dataquest 2.3 (Data Sciences International).

Hemodynamic Recording In Vivo. Anesthetized WT and mMCP-4(−/−) mice were cannulated via the left jugular vein (for intravenous administration of pharmacological agents) and the right carotid artery (for hemodynamic recording and blood sampling) with a 10-gauge polyethylene catheter.

The right carotid artery catheter was then connected to a Blood Pressure Analyzer 200A (Micro-Med, Tustin, CA) for arterial pressure measurements. The mice were allowed a 15-minute stabilization period before the intravenous injection of Big-ET-1, ET-1 (1–31), or ET-1 (Peptide Institute) at doses ranging from 0.001 to 10 nmol/kg. Data were then collected for 20 minutes before mice were killed.

In another series of experiments, specific inhibitors of the ECE [CGS 35066 (α-[(*S*)-(Phosphonomethyl)amino]-3-dibenzofuranpropanoic acid); 0.1 mg/kg i.v.] (Tocris Bioscience, Bristol, UK), chymase

(TY-51469; 20 mg/kg i.v.), or NEP (thiorphan; 2.5 mg/kg i.v.) (Sigma-Aldrich) were administered to the mice 20 minutes prior the injection of Big-ET-1 or ET-1 (1–31) (1 nmol/kg).

Measurement of Plasmatic Immunoreactive-ET-1 (1–31) and Immunoreactive-ET-1 after Big-ET-1 Administration In Vivo. WT and mMCP-4(−/−) mice were cannulated as described above. After a stabilization period, Big-ET-1 (1 nmol/kg) or ET-1 (1–31) (0.1 nmol/kg) was administered. A pretreatment of WT mice with CGS 30566 (0.1 mg/kg i.v.) was also performed 20 minutes prior to Big ET-1 (1 nmol/kg) administration. After a 1-minute time lapse, blood was collected and plasma was prepared by centrifugation.

The plasma samples were purified by HPLC as described above. As the concentrations are not high enough for direct HPLC detection, high concentration pure standards were used for each experiment to select the appropriate elution fractions for subsequent enzyme immunoassay (EIA) dosages.

The collected fractions were then dried overnight in a vacuum concentrator, and the measuring of immunoreactive (IR)-ET-1 and IR-ET-1 (1–31) was done using EIA kits from Immuno-Biologic Laboratories Co (Fujioka, Japan) according to the manufacturer's instructions.

Measurement of Endogenous Tissue IR-ET-1. The lungs, heart, aorta, and kidneys from WT and mMCP-4(−/−) mice were collected, homogenized, then purified on a DSC-18 solid phase extraction column (Supelco, Bellefonte, PA) and eluted with acetonitrile. The IR-ET-1 was measured by EIA as described above.

Statistical Analysis. All data are presented as mean ± S.E.M. Statistical significance was reached when the value of P was below 0.05 and based on the Student's t test performed with the GraphPad Instat 3.0 software (GraphPad Software, La Jolla, CA).

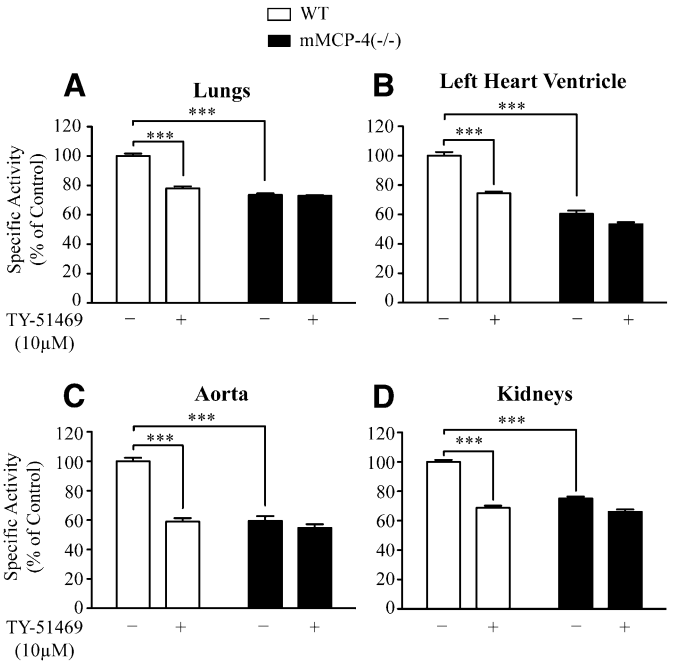

Fig. 1. Chymase-like enzymatic activity in the soluble fraction of lung (A), left heart ventricle (B), aorta (C) and kidney (D) homogenates from WT or mMCP-4(−/−) mice, treated with either vehicle (PBS) or a specific chymase inhibitor (TY-51469). ***$P < 0.001$; $n = 6$.

Results

Expression of ET-1 Generating Enzymes in mMCP-4(−/−) Mice. We evaluated the mRNA levels of ECE-1a, neprilysin (NEP), mMCP-1 and CPA1 in the lungs, left cardiac ventricle, aorta, and kidneys of WT and mMCP-4(−/−) mice by real-time reverse-transcription-PCR (Supplemental Table 3). The mRNA expression of ET-1 generating enzymes, ECE-1a and NEP, was not significantly different in mMCP-4(−/−) mice compared with their WT controls. The same was true for another mast cell protease with chymase activity, mMCP-1. In contrast, the mRNA expression of CPA1, a protease involved in ET-1 degradation, was elevated in mMCP-4(−/−) mice in the left cardiac ventricle (1.63 ± 0.17, $P = 0.014$) and the aorta (2.44 ± 0.37, $P = 0.012$) but not in the lungs (0.72 ± 0.66, $P = 0.689$) or the kidneys (1.27 ± 0.55, $P = 0.644$).

Reduced Chymase-Like Activity in mMCP-4(−/−) Mice Tissue Homogenates. The chymase-like activity in soluble fractions of tissue homogenates derived from WT and mMCP-4(−/−) mice is shown in Fig. 1. In all four organs tested, the basal chymase-like activity was significantly lower in the tissues of mMCP-4(−/−) mice than from their WT congeners. Moreover, the specific chymase inhibitor TY-51469 significantly reduced the chymase-like activity in WT mice down to the level of that found in corresponding samples from mMCP-4(−/−) mice, but had no effect on residual chymase-like activity in extracts from tissues of mMCP-4(−/−) mice.

Absence of In Vitro Conversion of Big-ET-1 to ET-1 (1–31) in mMCP-4(−/−) Mice. Figure 2 shows a typical experiment of the in vitro conversion of Big-ET-1 to ET-1 (1–31) in soluble fractions from lung homogenates derived from WT (with either vehicle or TY-51469) and mMCP-4(−/−) mice. The result of the conversion was purified by HPLC, and the Big ET-1 and ET-1 (1–31) peaks were isolated and verified by MS. Figure 2 shows that conversion of Big ET-1 to ET-1 (1–31) occurred in homogenates from WT lungs, but not homogenates treated with TY-51469 or from mMCP-4(−/−) mice. Supplemental Figure 3 shows the HPLC traces of these experiments. Similar results were obtained from the left cardiac ventricle, the aorta, and the kidneys (unpublished data).

Figure 3 shows the HPLC quantification of the conversion in the lung, left heart ventricle, aorta, and kidney homogenates. In soluble fractions from all four organs, conversion of Big-ET-1 to ET-1 (1–31) occurred in tissues from WT mice but not in tissues from WT mice pretreated with TY-51469 or in

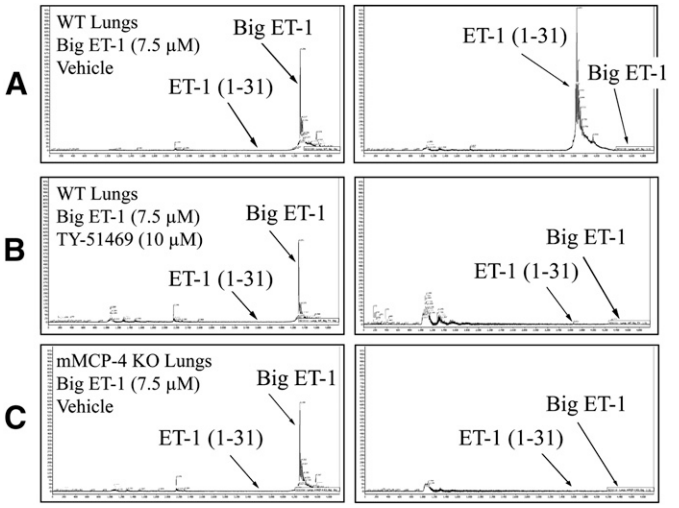

Fig. 2. In vitro conversion of Big-ET-1 to ET-1 (1–31) in soluble fractions from lung homogenates, with HPLC-MS identification of conversion results from WT (A), mMCP-4(−/−) (B), and WT tissues treated with TY-51469 (C).

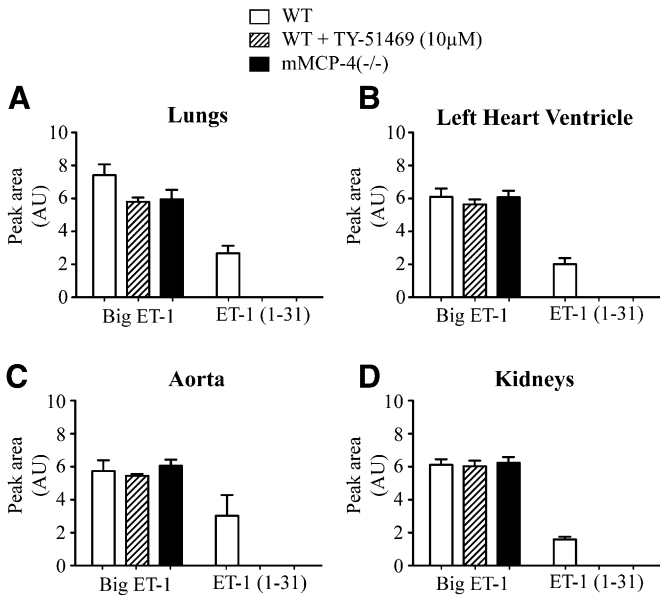

Fig. 3. Quantification of the in vitro conversion of Big ET-1 to ET-1 (1–31) in homogenates from the lungs (A), left heart ventricle (B), aorta (C), and kidneys (D) from WT (treated with vehicle or TY-51469) or mMCP-4(−/−) mice using HPLC area under the curve arbitrary units (AU); $n = 5$.

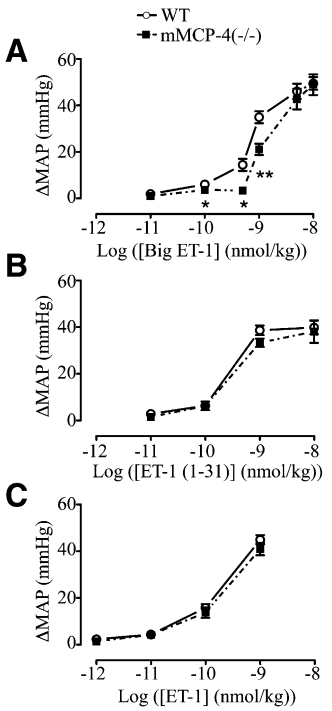

Fig. 4. Maximal variation in mean arterial pressure (△MAP) following the intravenous administration of Big-ET-1 (A), ET-1 (1–31) (B), and ET-1 (C) in WT and mMCP-4(−/−) mice. *$P < 0.05$; **$P < 0.01$; $n = 6$.

tissues derived from mMCP-4(−/−) mice. Big-ET-1 levels were similar in all conditions tested, indicating that the nonspecific degradation of Big-ET-1 in the soluble fraction of organs was not significantly affected by the absence of chymase activity in our experimental settings.

No Difference in Basal Hemodynamic Parameters in WT and mMCP-4(−/−) Mice. Prior to drug injection, the basal hemodynamic parameters were monitored in all cannulated mice. There was no difference in mean arterial pressure or heart rate between anesthetized WT and mMCP-4(−/−) mice (data not shown). Furthermore, the radiotelemetry experiment revealed that the mean arterial pressure was similar in both groups (103.2 ± 0.6 versus 108.7 ± 4.9 mmHg). The mean, systolic, and diastolic arterial pressures along with the arterial pulse pressure and the heart rate were similar in both groups and are reported in Supplemental Fig. 2.

Reduced Potency of Big-ET-1 in mMCP-4(−/−) Mice. We compared the in vivo dose-response curves for mean arterial pressure increase after the intravenous administration of Big-ET-1, ET-1 (1–31), or ET-1 in WT and mMCP-4(−/−) mice. ET-1 (1–31) and ET-1 elicited similar responses in WT and mMCP-4(−/−) mice at each dose used (Fig. 4, B and C). However, at doses of 0.1, 0.5, and 1.0 nmol/kg, the pressor response to Big-ET-1 was significantly reduced in mMCP-4(−/−) mice compared with WT mice (Fig. 4A).

The Residual Response to Big-ET-1 Is Insensitive to Chymase and NEP Inhibition in mMCP-4(−/−) Mice. Figure 5 shows the increase of mean arterial pressure induced over time by Big-ET-1 or ET-1 (1–31) (1 nmol/kg) in WT and mMCP-4(−/−) mice following systemic administration of either vehicle, CGS 35066, TY-51469, or thiorphan. The chymase inhibition by TY-51469 and the NEP inhibition by thiorphan effectively blunted the response to Big-ET-1 in WT mice but were ineffective in mMCP-4(−/−) mice, whereas ECE inhibition by CGS 35066 reduced the pressor response to Big ET-1 by 45% in WT mice and abolished the residual response to the precursor in mMCP-4(−/−) mice. In contrast, TY-51469 did not affect the response to ET-1 (1–31) in WT or mMCP-4(−/−) mice, and thiorphan blocked the pressor response to ET-1 (1–31) in both types of mice.

Reduced In Vivo Generation of IR-ET-1 (1–31) and IR-ET-1 in mMCP-4(−/−) Mice after Big-ET-1 Administration. Figure 6 shows the plasma levels of IR ET-1 and ET-1 (1–31) following intravenous administration of Big-ET-1 (1 nmol/kg) or ET-1 (1–31) (0.1 nmol/kg). Significantly lower levels of IR-ET-1 (1–31) were detected in plasma of mMCP-4(−/−) mice compared with their WT controls after Big-ET-1 administration. However, no difference in the plasma levels of IR-ET-1 (1–31) was detected after administration of ET-1 (1–31). Furthermore, a similar reduction was observed in the plasma levels of IR-ET-1 in mMCP-4(−/−) mice compared with their WT congeners. ECE inhibition reduced the plasma levels of IR-ET-1 by more than 40% following Big ET-1 administration in WT mice (without CGS 35066: 833.9 ± 91.9 fmol/ml; in presence of CGS 35066: 434.5 ± 46.5 fmol/ml, $P < 0.05$, $n = 5$–7 experiments) but not in mMCP-4(−/−) mice (468.8 ± 73.9 fmol/ml, $n = 6$).

Reduced Endogenous IR-ET-1 Levels in the Lungs of mMCP-4(−/−) Mice. Finally, Fig. 7 shows tissue IR-ET-1 levels in soluble fractions derived from lungs, left cardiac ventricle, aorta, and kidneys of WT or mMCP-4(−/−) mice. No significant differences in endogenous IR-ET-1 levels were observed in the left cardiac ventricle, the aorta, or the kidneys. However, significant reductions in IR-ET-1 levels were observed in lungs of mMCP-4(−/−) mice compared with lungs from WT controls. Furthermore, no significant differences were detected in baseline plasma IR-ET-1 levels between WT and mMCP-4(−/−) mice (5.2 ± 0.7 fmol/ml, $n = 7$ versus 6.8 ± 1.8 fmol/ml, $n = 8$).

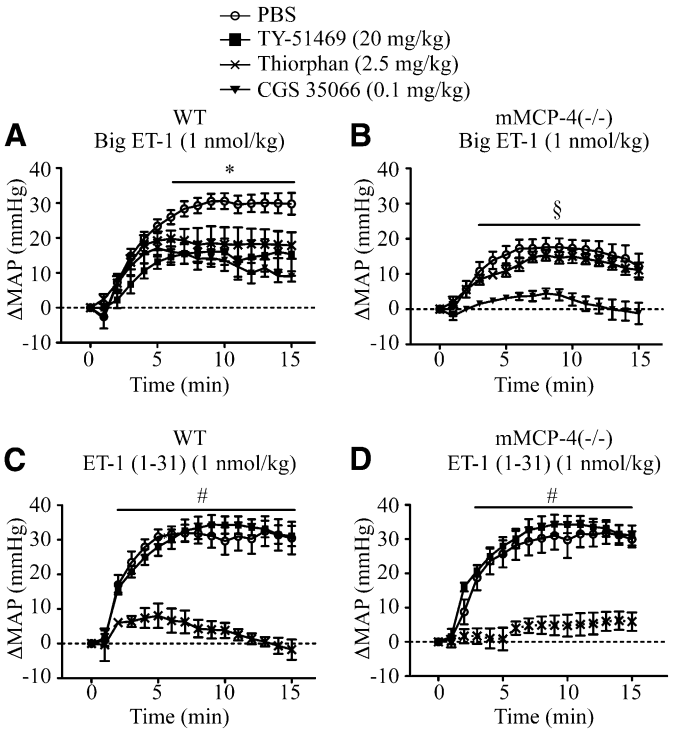

Fig. 5. Time course of the variation of the mean arterial pressure (△MAP) in response to i.v. administration of Big ET-1 (1 nmol/kg) [(A) WT mice; (B) mMCP-4(−/−) mice] or ET-1 (1-31) (1 nmol/kg) [(C) WT mice; (D) mMCP-4(−/−) mice] in mice pre-treated with either a chymase (TY-51469), a NEP (thiorphan) or an ECE inhibitor (CGS 35066). *$P < 0.05$ vs. PBS; #$P < 0.05$ vs. thiorphan; §$P < 0.05$ vs. CGS 35066; n = 5–9.

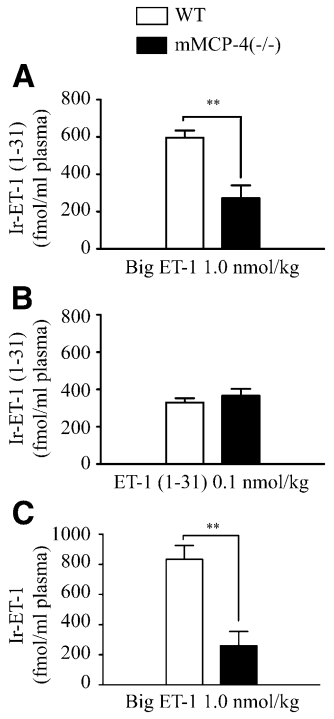

Fig. 6. In vivo conversion of Big-ET-1 into ET-1 (1–31) and ET-1 in WT and mMCP-4(−/−) mice. Quantification of the plasma levels of immunoreactive endothelin-1 (1–31) (A) and IR-ET-1 (C) after the intravenous administration of Big-ET-1 1.0 nmol/kg. In (B), the plasma levels of IR-ET-1 (1–31) were determined following the intravenous administration of ET-1 (1–31) (0.1 nmol/kg). **$P < 0.01$; n = 5–6.

Discussion

The present study demonstrates a pivotal role for mMCP-4 in the pressor properties of Big-ET-1, in the conversion of the latter to the intermediate peptide ET-1 (1–31) in vitro and in vivo, and in the pulmonary production of endogenous ET-1.

These results suggest that in addition to the endogenous ECE (McMahon et al., 1991), mouse mast cell chymase (mMCP-4) significantly contributes to the overall production of the potent pressor peptide ET-1 in the mouse model. mMCP-4(−/−) mice, compared with WT controls, show a 50% reduction in the pressor response and a marked decrease in plasma levels of both ET-1 (1–31) and ET-1 after systemic Big-ET-1 administration. Yet, in accordance with Groschwitz and colleagues (2009), we show that the basal blood pressure does not differ between conscious WT and mMCP-4(−/−) mice. Accordingly, the baseline plasma ET-1 levels did not vary between WT and mMCP-4(−/−). In addition, the specific inhibition of chymase (with TY-51469) and of NEP 24.11 (with thiorphan), reduced the pressor response to Big-ET-1 in WT mice but did not affect the residual response in mMCP-4(−/−) mice. Specific ECE inhibition with CGS 35066 reduced the pressor response to Big ET-1 in a similar fashion in both groups and further inhibited the residual response to the 38 amino acid precursor in mMCP-4(−/−) mice, whereas both groups responded equally to ET-1 (1–31) administration. Our group previously showed the dual contribution of both chymase and NEP in the in vivo conversion of Big-ET-1 to ET-1 in WT mice (Simard et al., 2009).

In the present study we also demonstrate for the first time that the genetic interruption of the mMCP-4 gene is sufficient to reduce the dynamic production of ET-1 (1–31) and ET-1 after systemic administration of Big-ET-1 and that ECE specific blockade reduced the plasma level increase of ET-1 by 50% in WT mice but could not further reduce ET-1 levels in mMCP-4(−/−) mice. These results are concordant with previously reported data from our laboratory showing that a chymase inhibitor, Suc-Val-Pro-Phe^{P}(OPh)$_2$, inhibited by over 60% the pressor response of Big ET-1 and reduced the plasma level increases of ET-1 by close to 90% in WT mice in vivo (Simard et al., 2009). Although this does not prove conclusively of a more important role of chymase versus ECE

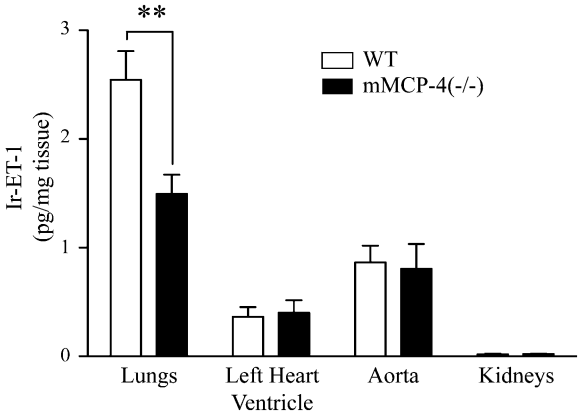

Fig. 7. Endogenous tissue levels of IR-ET-1 in the lungs, left cardiac ventricle, the aorta, and the kidneys. **$P < 0.05$; n = 6–7.

in ET-1 biosynthesis, because plasma ET-1 is mostly a spillover from endothelial basolateral metabolism, it still highlights an important role for chymase in the processing of Big ET-1 in the mouse model. One cannot exclude, in addition, adaptation mechanisms afforded by the genetic deletion of the mMCP-4 gene in the mouse model.

Pharmacological inhibition of chymase in WT mice with systemically administered Suc-Val-Pro-Phe$^{P}(OPh)_2$ or in the present study with TY-51469 or via the genetic deletion of mMCP-4 reduced the pressor responses to Big ET-1 to the same extent. In addition, we also showed that the genetic deletion of mMCP-4 reduced the increase of plasmatic ET-1 by more than 60% after the systemic administration of Big ET-1. We therefore suggest that the residual ET-1 plasma concentrations measured in mMCP-4(−/−) mice after Big-ET-1 administration represent a spillover produced by other enzymes with no currently identified significance in the overall cardiovascular effects of Big-ET-1 in the mouse in vivo. For example, matrix metalloproteinase-2 (MMP-2) can also cleave Big-ET-1 to generate ET-1 (1–32) (Fernandez-Patron et al., 1999). Whether the MMP-2-generated ET-1 (1–32) requires further C-terminal amino acid hydrolysis to elicit pharmacological effects remains to be investigated. Thus, pathways other than mMCP-4 may be involved in ET-1 (1–31) generation in vivo, but it is yet to be defined whether they have any significant role in the endothelin system in the mouse under normal conditions.

In addition, an HPLC/MALDI-MS approach demonstrated that the soluble fraction of either lung, cardiac, aortic, or renal tissue extracts derived from mMCP-4(−/−) mice do not have, in contrast to those from WT mice, the capacity to generate ET-1 (1–31) from Big-ET-1. It is also of interest that in this series of experiments, the specific chymase inhibitor TY-51469 (Koide et al., 2003; Palaniyandi et al., 2007) abolished the ET-1 (1–31) producing capacity of soluble fractions of several organs (lungs, left cardiac ventricle, aorta, kidney) derived from WT mice. These data strongly argue in favor of a pivotal role for mMCP-4 in the in vitro production of ET-1 (1–31) in the lungs, left cardiac ventricle, aorta, and kidney, all organs with significant ET-1 and chymase activity (Thorin and Clozel, 2010; Takai et al., 2011). Noteworthy, no conversion to mature ET-1 was detected by either HPLC or MALDI-MS in any of the samples tested. This lack of processing of either Big-ET-1 or ET-1 (1–31) to ET-1 in these experimental settings can be explained by the fact that both ECE and NEP, unlike mMCP-4, are membrane bound entities (McMahon et al., 1991) and therefore should be found in insignificant quantities in soluble fractions. The loss of Big-ET-1 conversion capacity of soluble extracts from vascular and nonvascular tissues of mMCP-4(−/−) mice is correlated with the absence of chymase inhibitor sensitive hydrolysis of the fluorogenic substrate Suc-Leu-Leu-Val-Tyr-AMC in the same preparations. We previously showed that soluble extracts from aorta, left ventricle, and lungs of WT mice hydrolyze the fluorogenic peptide via a chymase-sensitive but not an ECE-sensitive pathway (McMahon et al., 1991; Simard et al., 2009).

Finally, the total pulmonary content of endogenous ET-1 is markedly reduced in mMCP-4(−/−) mice compared with WT controls. It is well established that the pulmonary system accounts for 40% of all vascular endothelial cells, which are the main source of vascular ET-1 (Milnor, 1989). We therefore suggest that, in the NEP-rich pulmonary system (Baraniuk et al., 1995), mMCP-4-dependent synthesis of ET-1 accounts for a significant part of the overall endothelin production in the mouse. This particular state of events may explain the relative discrepancy of these results with the mMCP-4-to-ECE mRNA ratio between the lungs, heart, and aorta, where our previous study showed a smaller mMCP-4-to-ECE ratio in the lungs compared with the heart and the aorta (Simard et al., 2009).

In agreement with Yanagisawa et al. (2000), who suggested that proteases other than ECE may account for the genesis of ET-1 in the mouse, our data advocate for a pivotal contribution of the mMCP-4 in the non-ECE-dependent tissue production of ET-1 in the murine model. Our data are also in line with the finding that chymostatin is more efficient than phosphoramidon in blocking the extracellular conversion of Big-ET-1 to ET-1 in perfused rat lung (Wypij et al., 1992). As such, the pharmacological inhibition of chymase might provide an interesting alternative to ECE inhibitors and ET receptors antagonists. It would also have the added beneficial effects of inhibiting both ET-1 and Ang-II production directly at mast cell-infiltrated sites. The ET-1 and Ang-II systems are complimentary and potent inducers of each other, and both play crucial roles in a large number of biologic systems, such as the vasculature, heart, lungs, and the kidneys (Montanari et al., 2003; Davenport and Maguire, 2006; Paul et al., 2006). ET-1 and Ang-II can also induce the expression of fibrogenic factors such as transforming growth factor-β1 (Leask, 2010) and MMP-9 (Rouet-Benzineb et al., 2000; Ergul et al., 2003), which are themselves enzymatically activated by chymase (Takai et al., 2010). ET-1 can itself induce mast cell degranulation, thereby releasing chymase in the interstitium in a positive feedback loop (Walsh et al., 2009). Hence, chymase inhibition could have a tremendous effect on the ET-1 and Ang-II systems and their activities.

In vitro studies show that human chymase cleaves Big ET-1 to ET-1 (1–31) (Hanson et al., 1997; Nakano et al., 1997), but there are no data regarding the relevance of chymase-dependent synthesis of ET-1 in humans. However, recent studies show the beneficial impact of chymase inhibitors, or the genetic deletion of mMCP-4, in a number of animal models of disease (Jin et al., 2003; Takai et al., 2003; Tsunemi et al., 2004; Sun et al., 2009; Pejler et al., 2010), suggesting that study of chymase-dependent synthesis of ET-1 in human physiopathology warrants investigation. Finally, it is of interest that, unlike the genetic deletion of the ECE (Yanagisawa et al., 2000), the deletion of the mMCP-4 gene is not as deleterious, as mMCP-4(−/−) mice breed and develop normally, with only minor intestinal anomalies (Tchougounova et al., 2003; Groschwitz et al., 2009).

In conclusion, our study demonstrates that the serine protease mMCP-4 is importantly involved in the conversion and thus the biologic activity of Big-ET-1 in the mouse. In cardiovascular diseases, in which inflammatory processes and mast cell degranulation occur, chymase inhibitors may ultimately lead to the reduction of intramural production of not only Ang-II but ET-1 as well and thus reduce many of the downstream pathologic consequences.

Acknowledgments

The authors thank Adel Giaid and Élie Simard for useful discussion, Robert Day and Witold Neugebauer for the use of an ultraviolet-light plate reader and MALDI-Time of Flight mass spectrometer, and Fernand Gobeil, Jr., for the use of an Agilent Technology HPLC system. TY-51469 was graciously provided by Toa Eiyo Ltd.

Authorship Contributions

Participated in research design: Houde, Labonté, D'Orléans-Juste.

Conducted experiments: Houde, Labonté, Desbiens, Jamain, D'Orléans-Juste.

Contributed new reagents or analytic tools: Pejler, Gurish, Takai, D'Orléans-Juste.

Performed data analysis: Houde, Labonté, D'Orléans-Juste.

Wrote or contributed to the writing of the manuscript: Houde, Labonté, Pejler, Gurish, Takai, D'Orléans-Juste.

References

Andersson MK, Karlson U, and Hellman L (2008) The extended cleavage specificity of the rodent beta-chymases rMCP-1 and mMCP-4 reveal major functional similarities to the human mast cell chymase. *Mol Immunol* **45**:766–775.

Arai H, Hori S, Aramori I, Ohkubo H, and Nakanishi S (1990) Cloning and expression of a cDNA encoding an endothelin receptor. *Nature* **348**:730–732.

Baraniuk JN, Ohkubo K, Kwon OJ, Mak J, Ali M, Davies R, Twort C, Kaliner M, Letarte M, and Barnes PJ (1995) Localization of neutral endopeptidase (NEP) mRNA in human bronchi. *Eur Respir J* **8**:1458–1464.

Butz GM and Davisson RL (2001) Long-term telemetric measurement of cardiovascular parameters in awake mice: a physiological genomics tool. *Physiol Genomics* **5**:89–97.

Carlson SH and Wyss JM (2000) Long-term telemetric recording of arterial pressure and heart rate in mice fed basal and high NaCl diets. *Hypertension* **35**:E1–E5.

Caughey GH (2007) Mast cell tryptases and chymases in inflammation and host defense. *Immunol Rev* **217**:141–154.

D'Orléans-Juste P, Houde M, Rae GA, Bkaily G, Carrier E, and Simard E (2008) Endothelin-1 (1-31): from chymase-dependent synthesis to cardiovascular pathologies. *Vascul Pharmacol* **49**:51–62.

D'Orléans-Juste P, Plante M, Honoré JC, Carrier E, and Labonté J (2003) Synthesis and degradation of endothelin-1. *Can J Physiol Pharmacol* **81**:503–510.

Davenport AP and Maguire JJ (2006) Endothelin. *Handb Exp Pharmacol* **176**: 295–329.

Denault JB, Claing A, D'Orléans-Juste P, Sawamura T, Kido T, Masaki T, and Leduc R (1995) Processing of proendothelin-1 by human furin convertase. *FEBS Lett* **362**: 276–280.

Ergul A, Portik-Dobos V, Giulumian AD, Molero MM, and Fuchs LC (2003) Stress upregulates arterial matrix metalloproteinase expression and activity via endothelin A receptor activation. *Am J Physiol Heart Circ Physiol* **285**:H2225–H2232.

Fecteau M-H, Honoré J-C, Plante M, Labonté J, Rae GA, and D'Orléans-Juste P (2005) Endothelin-1 (1-31) is an intermediate in the production of endothelin-1 after big endothelin-1 administration in vivo. *Hypertension* **46**:87–92.

Fernandez-Patron C, Radomski MW, and Davidge ST (1999) Vascular matrix metalloproteinase-2 cleaves big endothelin-1 yielding a novel vasoconstrictor. *Circ Res* **85**:906–911.

Fleming I (2006) Signaling by the angiotensin-converting enzyme. *Circ Res* **98**:887–896.

Groschwitz KR, Ahrens R, Osterfeld H, Gurish MF, Han X, Abrink M, Finkelman FD, Pejler G, and Hogan SP (2009) Mast cells regulate homeostatic intestinal epithelial migration and barrier function by a chymase/Mcpt4-dependent mechanism. *Proc Natl Acad Sci USA* **106**:22381–22386.

Hanson GC, Andersson KE, Gyllstedt E, Högestätt ED, and Lindberg BF (1997) Hydrolysis of big endothelin-1 by a serine protease in the membrane fraction of human lung. *Regul Pept* **68**:63–69.

Hayasaki-Kajiwara Y, Naya N, Shimamura T, Iwasaki T, and Nakajima M (1999) Endothelin generating pathway through endothelin1-31 in human cultured bronchial smooth muscle cells. *Br J Pharmacol* **127**:1415–1421.

Inoue N, Muramatsu M, Jin D, Takai S, Hayashi T, Katayama H, Kitaura Y, Tamai H, and Miyazaki M (2009) Effects of chymase inhibitor on angiotensin II-induced abdominal aortic aneurysm development in apolipoprotein E-deficient mice. *Atherosclerosis* **204**:359–364.

Jin D, Takai S, Yamada M, Sakaguchi M, Kamoshita K, Ishida K, Sukenaga Y, and Miyazaki M (2003) Impact of chymase inhibitor on cardiac function and survival after myocardial infarction. *Cardiovasc Res* **60**:413–420.

Kaartinen M, Penttilä A, and Kovanen PT (1994) Accumulation of activated mast cells in the shoulder region of human coronary atheroma, the predilection site of atheromatous rupture. *Circulation* **90**:1669–1678.

Koide Y, Tatsui A, Hasegawa T, Murakami A, Satoh S, Yamada H, Kazayama S, and Takahashi A (2003) Identification of a stable chymase inhibitor using a pharmacophore-Based database search. *Bioorg Med Chem Lett* **13**:25–29.

Leask A (2010) Potential therapeutic targets for cardiac fibrosis: TGFbeta, angiotensin, endothelin, CCN2, and PDGF, partners in fibroblast activation. *Circ Res* **106**:1675–1680.

Mangiapane ML, Rauch AL, MacAndrew JT, Ellery SS, Hoover KW, Knight DR, Johnson HA, Magee WP, Cushing DJ, and Buchholz RA (1994) Vasoconstrictor action of angiotensin I-convertase and the synthetic substrate (Pro11,D-Ala12)-angiotensin I. *Hypertension* **23**:857–860.

Mawatari K, Kakui S, Harada N, Ohnishi T, Niwa Y, Okada K, Takahashi A, Izumi K, and Nakaya Y (2004) Endothelin-1(1-31) levels are increased in atherosclerotic lesions of the thoracic aorta of hypercholesterolemic hamsters. *Atherosclerosis* **175**: 203–212.

McMahon EG, Palomo MA, Moore WM, McDonald JF, and Stern MK (1991) Phosphoramidon blocks the pressor activity of porcine big endothelin-1-(1-39) in vivo and conversion of big endothelin-1-(1-39) to endothelin-1-(1-21) in vitro. *Proc Natl Acad Sci USA* **88**:703–707.

Milnor WR (1989) *Hemodynamics*, Williams & Wilkins, Baltimore, MD.

Montanari A, Biggi A, Carra N, Ziliotti M, Fasoli E, Musiari L, Perinotto P, and Novarini A (2003) Endothelin-A receptors mediate renal hemodynamic effects of exogenous Angiotensin II in humans. *Hypertension* **42**:825–830.

Nakano A, Kishi F, Minami K, Wakabayashi H, Nakaya Y, and Kido H (1997) Selective conversion of big endothelins to tracheal smooth muscle-constricting 31-amino acid-length endothelins by chymase from human mast cells. *J Immunol* **159**: 1987–1992.

Palaniyandi SS, Nagai Y, Watanabe K, Ma M, Veeraveedu PT, Prakash P, Kamal FA, Abe Y, Yamaguchi K, and Tachikawa H, et al. (2007) Chymase inhibition reduces the progression to heart failure after autoimmune myocarditis in rats. *Exp Biol Med (Maywood)* **232**:1213–1221.

Paul M, Poyan Mehr A, and Kreutz R (2006) Physiology of local renin-angiotensin systems. *Physiol Rev* **86**:747–803.

Pejler G, Rönnberg E, Waern I, and Wernersson S (2010) Mast cell proteases: multifaceted regulators of inflammatory disease. *Blood* **115**:4981–4990.

Pfaffl MW (2001) A new mathematical model for relative quantification in real-time RT-PCR. *Nucleic Acids Res* **29**:e45.

Rouet-Benzineb P, Gontero B, Dreyfus P, and Lafuma C (2000) Angiotensin II induces nuclear factor- kappa B activation in cultured neonatal rat cardiomyocytes through protein kinase C signaling pathway. *J Mol Cell Cardiol* **32**:1767–1778.

Sakurai T, Yanagisawa M, Takuwa Y, Miyazaki H, Kimura S, Goto K, and Masaki T (1990) Cloning of a cDNA encoding a non-isopeptide-selective subtype of the endothelin receptor. *Nature* **348**:732–735.

Simard E, Jin D, Takai S, Miyazaki M, Brochu I, and D'Orléans-Juste P (2009) Chymase-dependent conversion of Big endothelin-1 in the mouse in vivo. *J Pharmacol Exp Ther* **328**:540–548.

Sun J, Zhang J, Lindholt JS, Sukhova GK, Liu J, He A, Abrink M, Pejler G, Stevens RL, and Thompson RW, et al. (2009) Critical role of mast cell chymase in mouse abdominal aortic aneurysm formation. *Circulation* **120**:973–982.

Takai S, Jin D, and Miyazaki M (2010) Chymase as an important target for preventing complications of metabolic syndrome. *Curr Med Chem* **17**:3223–3229.

Takai S, Jin D, and Miyazaki M (2011) Targets of chymase inhibitors. *Expert Opin Ther Targets* **15**:519–527.

Takai S, Jin D, Sakaguchi M, Katayama S, Muramatsu M, Sakaguchi M, Matsumura E, Kim S, and Miyazaki M (2003) A novel chymase inhibitor, 4-[1-([bis-(4-methylphenyl)-methyl]-carbamoyl)3-(2-ethoxy-benzyl)-4-oxo-azetidine-2-yloxy]-benzoic acid (BCEAB), suppressed cardiac fibrosis in cardiomyopathic hamsters. *J Pharmacol Exp Ther* **305**:17–23.

Tchougounova E, Pejler G, and Abrink M (2003) The chymase, mouse mast cell protease 4, constitutes the major chymotrypsin-like activity in peritoneum and ear tissue. A role for mouse mast cell protease 4 in thrombin regulation and fibronectin turnover. *J Exp Med* **198**:423–431.

Thorin E and Clozel M (2010) The cardiovascular physiology and pharmacology of endothelin-1. *Adv Pharmacol* **60**:1–26.

Tsunemi K, Takai S, Nishimoto M, Jin D, Sakaguchi M, Muramatsu M, Yuda A, Sasaki S, and Miyazaki M (2004) A specific chymase inhibitor, 2-(5-formylamino-6-oxo-2-phenyl-1,6-dihydropyrimidine-1-yl)-N-[[3,4-dioxo-1-phenyl-7-(2-pyridyloxy)]-2-heptyl]acetamide (NK3201), suppresses development of abdominal aortic aneurysm in hamsters. *J Pharmacol Exp Ther* **309**:879–883.

Urata H, Boehm KD, Philip A, Kinoshita A, Gabrovsek J, Bumpus FM, and Husain A (1993) Cellular localization and regional distribution of an angiotensin II-forming chymase in the heart. *J Clin Invest* **91**:1269–1281.

Urata H, Kinoshita A, Misono KS, Bumpus FM, and Husain A (1990) Identification of a highly specific chymase as the major angiotensin II-forming enzyme in the human heart. *J Biol Chem* **265**:22348–22357.

Walsh SK, Kane KA, and Wainwright CL (2009) Mast cell degranulation—a mechanism for the anti-arrhythmic effect of endothelin-1? *Br J Pharmacol* **157**:716–723.

Wypij DM, Nichols JS, Novak PJ, Stacy DL, Berman J, and Wiseman JS (1992) Role of mast cell chymase in the extracellular processing of big-endothelin-1 to endothelin-1 in the perfused rat lung. *Biochem Pharmacol* **43**:845–853.

Yanagisawa H, Hammer RE, Richardson JA, Emoto N, Williams SC, Takeda Si, Clouthier DE, and Yanagisawa M (2000) Disruption of ECE-1 and ECE-2 reveals a role for endothelin-converting enzyme-2 in murine cardiac development. *J Clin Invest* **105**:1373–1382.

Yanagisawa M, Kurihara H, Kimura S, Tomobe Y, Kobayashi M, Mitsui Y, Yazaki Y, Goto K, and Masaki T (1988) A novel potent vasoconstrictor peptide produced by vascular endothelial cells. *Nature* **332**:411–415.

Yoshizumi M, Kim S, Kagami S, Hamaguchi A, Tsuchiya K, Houchi H, Iwao H, Kido H, and Tamaki T (1998) Effect of endothelin-1 (1-31) on extracellular signal-regulated kinase and proliferation of human coronary artery smooth muscle cells. *Br J Pharmacol* **125**:1019–1027.

Address correspondence to: Pedro D'Orléans-Juste, Département de Pharmacologie, 3001 12e Avenue Nord, Sherbrooke, Québec, Canada. E-mail: labpdj@usherbrooke.ca